

Poly(L-Lactic Acid)-Based Microcapsule Containing Phase-Change Material: Influence of Polymer Shell on Particle Morphology

Primprapa Sangjun¹ and Amorn Chaiyasat^{1,2*}

¹*Department of Chemistry, Faculty of Science and Technology, Rajamangala University of Technology Thanyaburi, Pathum Thani 12110, Thailand*

²*Advanced Materials Design and Development (AMDD) Research Unit, Faculty of Science and Technology, Rajamangala University of Technology Thanyaburi, Pathum Thani 12110, Thailand*

(Received March 7, 2019; Revised June 4, 2019; Accepted June 24, 2019)

Abstract: The preparation of poly(l-lactic acid) (PLLA)-based microcapsules containing phase change material Rubitherm 27 (RT27) by microsuspension polymerization was first developed. Before polymerization, a commercial PLLA was depolymerized via glycolysis to produce a shorter molecular chain as in PLLA glycosates (GPLLA). The influence of the polymer shell on particle morphology was studied by Optical microscope and Scanning electron microscope. The chemical structures of the obtained polymer microcapsule were characterized by Fourier-transform infrared spectroscopy and Nuclear magnetic resonance spectroscopy. The thermal properties and content of encapsulated RT27 were measured by Differential scanning calorimetry and Thermogravimetric analysis. Phase separation was clearly observed after droplet generation with methyl methacrylate, ethylene glycol dimethacrylate, and polyethylene glycol diacrylate as comonomers. After polymerization, broken particles were obtained. In contrast, a spherical microcapsule with a smooth surface was obtained with copolymerization between GPLLA and glycidyl methacrylate. In addition, high encapsulation efficiency (96 %) was obtained. The latent heats of encapsulated RT27 in the term of J/g-RT27 were 202 and 200 J/g-RT27 for the heat of melting and crystallization, respectively, which were close to those of the pristine RT27. Moreover, a supercooling phenomenon was not observed.

Keywords: Poly(l-lactic acid), Microcapsule, Phase change material, Microsuspension polymerization

Introduction

Phase-change, or heat storage, materials (PCMs) such as paraffin wax are extensively used in various applications such as temperature-adaptable greenhouses, thermal-adaptable fibers, solar heat storage, and air conditioning of buildings [1,2]. They have a wide range of melting and crystallization temperatures [3], have moderate energy capacities, are noncorrosive and are chemically inert. However, low thermal conductivity and leakage during phase transition are the main disadvantages of PCMs [4], which extremely limit their thermal energy storage applications [5-7]. To provide greater heat transfer and control volume change, PCMs are encapsulated within solid inorganic or organic shells. Based on high thermal stability and thermal conductivity, various inorganic shells such as calcium carbonate [8], silicon dioxide [9] and titanium dioxide [10] are used. However, when compared with polymeric shells, the encapsulation efficiency of such inorganic shell materials is low [11]. For the fabrication of PCM polymer microcapsules, various techniques are employed, such as interfacial polymerization [11], complex coacervation [12], and suspension polymerization [13] (including suspension-like [14] and microsuspension polymerizations [15-19]). Among the various techniques, suspension polymerization is useful for the preparation of microcapsules containing PCMs because of high encapsulation

efficiency and simply controlled synthesis. Various kinds of polymers shells are used to fabricate PCM microcapsules by suspension polymerization, such as polystyrene (PS) [20, 21], polydivinylbenzene (PDVB) [22], poly(styrene-co-divinylbenzene) [23], poly(methyl methacrylate) (PMMA) [17] and its copolymer [16,18]. However, microcapsule shells are usually synthesized from petrochemical-based monomers. Due to their nondegradable nature, there is a growing concern about their impact on the environment as waste contaminants [24,25].

Therefore, biodegradable polymers and sustainable materials have received considerable attention [26,27]. PLLA is one of the most famous biodegradable polymers, which are environmentally friendly, biocompatible, and nontoxic. It has been used in various applications such as the biomedical, pharmaceutical, food packaging, and agricultural industries [28,29]. Thus, PLLA is a good candidate for use as the polymer shell of PCM polymer microcapsules, into which little research has been done. From our previous work, we have successfully prepared a microcapsule with a commercial PLLA shell containing Vitamin E [30] and urea [31,32] in oil-in-water (O/W) and water-in-oil-in-water (W/O/W) emulsion systems, respectively, with a simple evaporation emulsion method. The PLLA shell represents high strength with comparatively high encapsulation efficiency (EE). Therefore, it should be possible to prepare a microcapsule containing wax using PLLA as a polymer shell. A commercial PLLA with high molecular weight was

*Corresponding author: a_chaiyasat@mail.rmutt.ac.th

also used as a microcapsule shell to encapsulate palmitic acid [33] and octadecane [34] as PCMs by solvent evaporation. However, a low percentage of EE was obtained in both cases, as the PLLA shell was not complete enough to envelop the PCMs. Because PLLA and PCMs have very different polarities and are miscible with dispersing dichloromethane solution, phase separation between the two components was formed as a Janus particle with different hemispheres during solvent evaporation. This finding accorded with the phenomenon of PS/PMMA blending using toluene, as was observed using a dispersing solution [35]. In addition, molecular weight increases the interfacial tension between the two components. Therefore, the utilization of low-molecular-weight PLLA should be studied. Glycolysis employing ethylene glycol is one of the simpler techniques to break PLLA chains [36,37] and results in low-molecular-weight PLLA. It is well known that shell strength decreases with the decrease in the molecular weight of a polymer shell. Thus, low-molecular-weight PLLA will be grafted with comonomer via radical polymerization to enhance microcapsule shell strength. To avoid multistep preparation, one-pot graft copolymerization onto PLLA chains is then considered. Benzoyl peroxide is one of the well-known peroxide initiators and contains an appropriate structure to abstract active hydrogen from polymer chains [38]. Based on the thermal decomposition of weak O-O bonds to form two highly active radicals (RO·), the obtained active radical then abstracted H atoms from polymer chains, presenting the active site on polymer chains for further reaction via radical polymerization.

In this research, microcapsules containing the commercial wax Rubitherm 27 (RT27) and PLLA-based microcapsule shells will be prepared via radical polymerization using BPO as an initiator in microsuspension polymerization. In addition, the influence of various kinds of hydrophilic comonomers such as glycidyl methacrylate (GMA), methyl methacrylate (MMA), ethylene glycol dimethacrylate (EGDMA), and polyethylene glycol acrylate (PEGDA) will be investigated for the formation of microcapsules, encapsulation efficiency, and colloidal stability of the microcapsules.

Experimental

Materials

PLLA with a molecular weight of 145,000 g/mol (B. C. Polymers Marketing Co., Ltd., Bangkok, Thailand), RT27 (Rubitherm technologies GmbH, Berlin, Germany commercial grade), Polyvinyl alcohol (PVA, degree of saponification 87-90 %; Aldrich, Milwaukee, Wisconsin, USA), Ethylene glycol (EG, purity 99.5 %; Loba Chemie Pvt. Ltd., India), chloroform (CHCl₃, purity 99.8 %; RCI Labscan, Bangkok, Thailand) and deuterated chloroform (CDCl₃, 99.8 %; Cambridge Isotope Laboratories, Inc., USA) were used as received. GMA (Aldrich, Wisconsin, USA; purity 99 %), MMA (Aldrich, Wisconsin, USA; purity 99 %), EGDMA (Aldrich, Wisconsin, USA; purity 99 %) and PEGDA (Aldrich, Wisconsin, USA; purity 99 %) were purified by passing through a column packed with basic aluminum oxide. Regent grade benzoyl peroxide (BPO; Merck, Munich, Germany) was purified by recrystallization in ethanol.

Microcapsule Preparation

Before microcapsule preparation, a commercial PLLA with a molecular weight of 145,000 g/mol was glycolyzed employing EG based on previous works [34,36] to obtain a shorter chain as a glycolyzed PLLA (GPLLA). Briefly, PLLA and EG at 1:1 weight ratio was mixed with chloroform (finally, 20 wt% of PLLA). Thereafter, the solution was transferred to a round-bottom flask and sealed with a silicone rubber septum. Before starting the reaction, the solution was purged with five vacuum/N₂ cycles finally in an N₂ atmosphere. The reaction was started at 175 °C with a mild stirring by magnetic stirrer and kept at 60 min. Finally, the obtained GPLLA was precipitated in methanol before further use.

GPLLA-based polymer microcapsules encapsulating RT27 were prepared by microsuspension polymerization under the conditions listed in Table 1. First, GPLLA was homogeneously mixed with a comonomer (various kinds of comonomer: GMA or MMA or EGDMA or PEGDA), BPO, and RT27 in chloroform as an oil phase. It was then poured into a

Table 1. Reagent amounts for the preparation of microcapsule containing RT27 by microsuspension polymerization^a

Phase	Chemicals	Various polymer shells			
		Run 1	Run 2	Run 3	Run 4
Oil	GPLLA (g)	2.50	1.25	1.50	2.00
	Comonomer (g)	-	1.25 ^b	1.00 ^c	0.50 ^c
	RT27 (g)	2.50	2.50	2.50	2.50
	BPO	-	0.25	0.25	0.25
	CHCl ₃ (g)	10.00	10.00	10.00	10.00
Aqueous	PVA solution (1 wt%) (g)	45.00	45.00	45.00	45.00

^aTemperature 55 °C, homogenized at 5000 rpm for 5 min and polymerization time 24 h, ^bGMA, MMA, EGDMA and PEGDA, and ^cGMA.

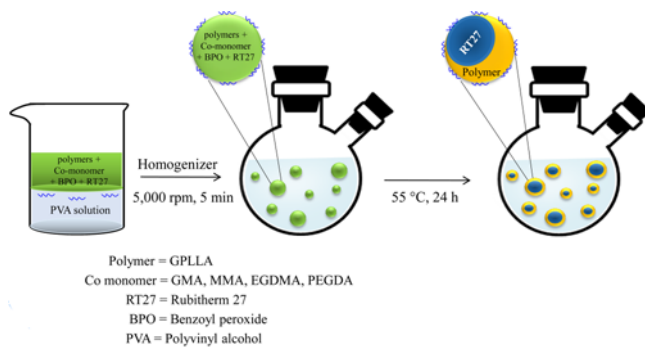


Figure 1. Schematic diagram for the preparation of microcapsule containing RT27 by microsuspension polymerization.

PVA aqueous solution (1 wt%) before being mechanical homogenized at 5,000 rpm for 5 min to form an oil-in-water emulsion. The obtained emulsion was subsequently transferred to a round-bottom flask and sealed with a silicone rubber septum. The suspension was purged with 5 vacuum/N₂ cycles finally in an N₂ atmosphere. The polymerization was started at 55 °C with a stirring rate of 500 rpm for 24 h. The schematic diagram of microcapsule preparation is shown in Figure 1. The control microcapsule using only GPLLA as a polymer shell was prepared without any polymerization, and the procedure was otherwise the same as microsuspension polymerization.

Characterization of PLLA Microcapsules

Microcapsule morphologies including inner structure, shape, and surface were observed by an optical microscope (OM; SK-100EB&SK-100ET, Seek, Seek Inter Co. Ltd., Thailand) and scanning electron microscope (SEM; JSM-6510, JEOL, JEOL Ltd., Japan). For SEM observation, a few dried microcapsules were distributed onto a nickel SEM stub and dried before Au-coating. Monomer conversion was measured by gravimetry. A suspension sample (~2.0 g) containing several drops of hydroquinone solution (1 wt%) in the aluminum cup was weighed before being evaporated in an oven at 70 °C. The sample was dried until the constant weight of the dried polymer was obtained. Based on comparing the weight of dried polymer with the original monomer, monomer conversion was then obtained. The molecular weight of the polymer was measured by gel permeation chromatography (GPC; Waters 2414, Waters, USA) with two poly(S/divinylbenzene) gel columns (Phenogel 5×103 and 5×105 Å (pores), 7.8 mm (i.d.)×30 cm (length), Phenomenex, USA) connected in a serie. The flow rate of THF as eluent was maintained at 1.0 ml/min with a column temperature of 40 °C, and elution was monitored with a refractive index detector (RI 2414/Waters). The columns were calibrated with six standard PS samples (2.5×10³-6.0×10⁵, M_w/M_n=1.05-1.15). Chemical structures were characterized by Fourier transform infrared spectrometer

(FTIR; Nicolet iS5, Thermo Scientific, USA) with a wavenumber range from 4,000 to 500 cm⁻¹ and Proton nuclear magnetic resonance spectroscopy (¹H NMR; PreCool ASC30, JEOL) at 400 MHz where CDCl₃ was used as a solvent. For FTIR measurement, dried samples were placed directly on the FTIR crystal. For ¹H NMR measurement, each sample (GPLLA, GMA, and purified GPLLA-g-PGMA) were dissolved in CDCl₃ before measurement. The RT27 content included in the microcapsules (percent experimental loading; %L_E (wt%)) was directly determined by the thermogravimetric analyzer (TGA; TGA 4000, Perkin-Elmer, USA) at a heating rate of 5 °C/min. Latent heats (ΔH_m and ΔH_c) (J/g-capsule) and the melting (T_m) and crystallization (T_c) temperatures of the encapsulated RT27 were measured with a differential scanning calorimeter (DSC; DSC 4000, Perkin-Elmer, USA) under an N₂ flow in a scanning temperature range of -20 to 40 °C with a heating/cooling rate of 5 °C/min. Before measurement by both TGA and DSC techniques, the microcapsules were washed with 2-propanol to remove unencapsulated RT27 on the microcapsule surface before being dried in a vacuum oven. Latent heats (ΔH_m^{*} and ΔH_c^{*}) of RT27 in the unit of J/g-RT27 and percent theoretical loading (%L_{th}) of RT27 in the washed microcapsules were calculated using equation (1) and equation (2), respectively. In addition, the encapsulation efficiency (%EE) of RT27 was calculated using equation (3).

$$\Delta H_m^* \text{ or } \Delta H_c^* = \left(\frac{\Delta H_m \text{ or } \Delta H_c}{\%L_E} \right) \times 100 \quad (1)$$

$$\%L_{th} = \left(\frac{W_{RT27}}{W_{RT27} + W_{GPLLA} + \left(W_M \times \frac{\%Conv}{100} \right)} \right) \times 100 \quad (2)$$

$$\%EE = \left(\frac{\%L_E}{\%L_{th}} \right) \times 100 \quad (3)$$

where, ΔH_m^{*} or ΔH_c^{*} is the latent heat of the encapsulated RT27 in a unit of joules per 1 g of encapsulated RT27 (J/g-RT27). ΔH_m or ΔH_c is the latent heat of the encapsulated RT27 in a unit of joules per 1 g of microcapsule (J/g-capsule) directly measured by DSC. %L_E is % experimental loading of RT27 in the washed microcapsules measured by TGA. W_{RT27}, W_{GPLLA}, and W_M are weights used in the recipe (Table 1) of RT27, GPLLA, and comonomers (GMA or MMA or EGDMA or PEGDA), respectively. %Conv is percent monomer conversion.

Results and Discussion

To achieve a microcapsule preparation containing RT27 by microsuspension polymerization, internal phase separation within the polymerizing particle is the main driving force where the polymer and RT27 were expected to be a shell and

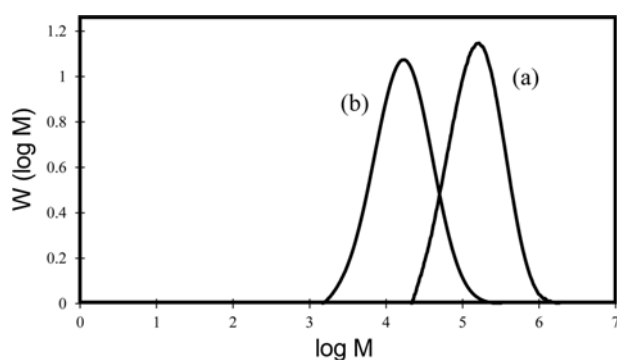


Figure 2. Overlaid molecular weight distribution curves of the commercial PLLA (a) and GPLLA (b) after glycolysis at 1 h.

core, respectively. Before polymerization, the monomer droplet containing PLLA, comonomer, and RT27 was homogeneous. Consequently, phase separation took place with an increase of polymer chain length where polymer chains were immiscible with the other components. The component representing lower interfacial tension with water (continuous phase) moved to the interface to become the shell and left the higher interfacial tension with water in the core. Therefore, the internal viscosity in the polymerizing particle affecting the mobility of the polymer chains is the main factor to attain the microcapsule formation. The commercial PLLA with a molecular weight of 145,000 g/mol was then depolymerized via glycolysis reaction. The molecular weight of PLLA had significantly decreased from 145,000 to 12,000 g/mol over a reaction time of 1 h. This is due to the depolymerization of PLLA by EG to form shorter chains of hydroxyl (OH)-terminated PLLAs called GPLLA [34,36]. The overlaid molecular weight distribution curves of the commercial PLLA and GPLLA are shown in Figure 2.

Microcapsules Prepared by a Simple Solvent Evaporation

Before microsuspension polymerization, microcapsule preparation was first tried with a simple solvent evaporation technique of GPLLA/RT27 droplets (in chloroform solution) generated by a homogenizer. The formed spherical GPLLA/RT27 droplets of a size greater than 10 μm were dispersed

in a continuous phase of PVA aqueous solution (1 wt%) as shown in Figure 3(a). After chloroform evaporation, a Janus structure in the form of dumbbell-like particles was clearly observed (Figure 3(b)). This means that two incompatible phases distinctly split into their own main domains of GPLLA-rich and RT27-rich while still portions of a single particle. Because the RT27-rich part, as the soft phase at room temperature, could not maintain its shape in a dried state, most of the RT27-rich part disappeared after redispersing the dried particle in the water phase (Figure 3(c)). This accorded with the SEM micrograph of the dried GPLLA/RT27 particles (Figure 3(d)), in which the crescent-shaped particles were mainly observed. In addition, the %EE of encapsulated RT27 was quite low at 62%. The copolymerization of GPLLA with a comonomer was then required to improve %EE.

Microcapsules Prepared by Microsuspension Polymerization

As a highly active radical ($\text{RO}\cdot$) initiated from BPO can abstract H atoms from the polymer chains, the main chain of the polymer would present the radically active site [38] for further polymerization. Therefore, a microcapsule containing RT27 with a shell of GPLLA copolymerized with some monomers by one-pot microsuspension polymerization employing BPO would achieve this aim. Various kinds of biocompatible comonomers including GMA, MMA, EGDMA, and PEGDA were used in microsuspension polymerization. After the droplet generation, internal phase separation was clearly observed with MMA, EGDMA and PEGDA comonomers (Figure 4(b)-(d)). Incomplete microcapsules (Figure 4(b')-(d')) as broken particles were mainly formed after polymerization. In addition, this phenomenon is clearly observed in SEM micrographs (Figure 5(b)-(d)) of the dried microcapsules. In contrast, using GMA comonomer, microcapsules without broken particles were smoothly formed (Figure 4(a') and 5(a)) even though partial heterogeneity was observed in oil droplets (Figure 4(a)). GMA may not only graft onto GPLLA chains, but also connect the end chain of GPLLA containing the OH group with an epoxide ring opening. The compatibility of both polymers might improve if the formed polymer shell provides higher

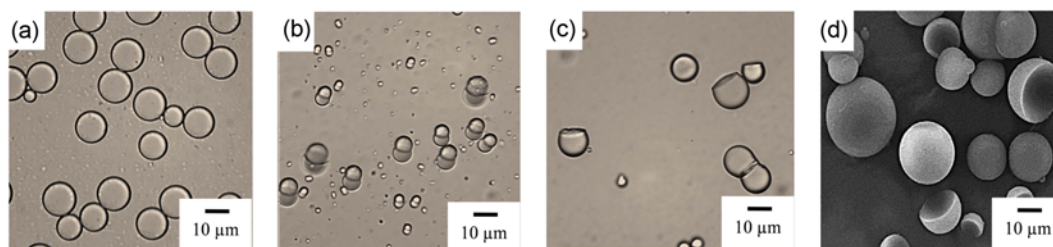


Figure 3. Optical micrographs (a-c) of GPLLA/RT27 droplets before (a), after (b) solvent evaporation and dried particles re-dispersed in water (c) and SEM photograph of dried GPLLA/RT27 particles (d).

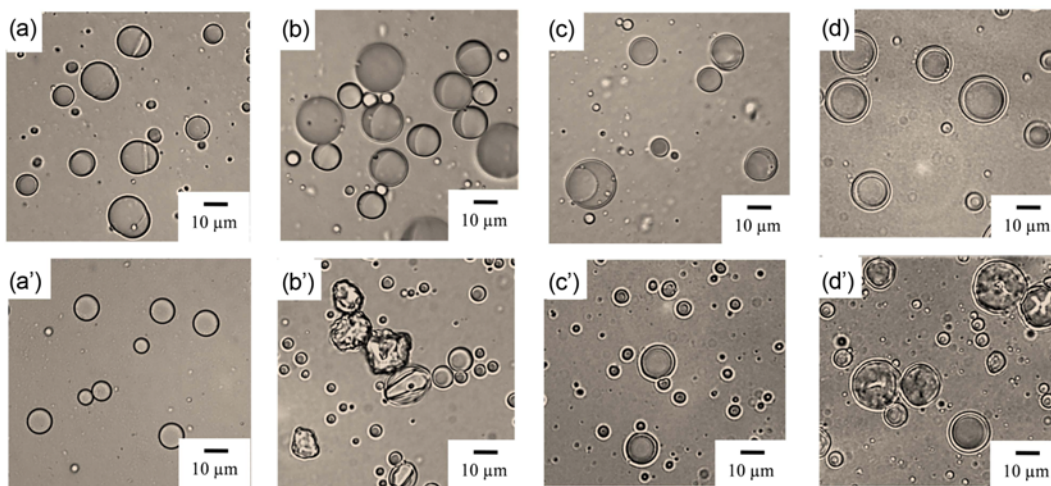


Figure 4. Optical micrographs of monomer droplets (a-d) and microcapsules containing RT27 (a'-d') prepared by microsuspension polymerization using various comonomers; (a, a') GMA, (b, b') MMA, (c, c') EGDMA, and (d, d') PEGDA.

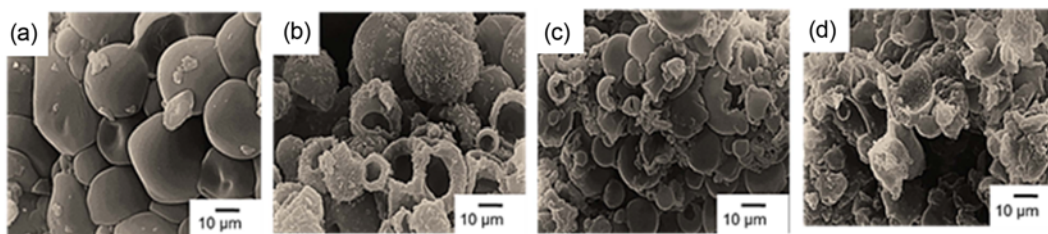


Figure 5. SEM micrographs of microcapsules containing RT27 prepared by microsuspension polymerization using various comonomers; (a) GMA, (b) MMA, (c) EGDMA, and (d) PEGDA.

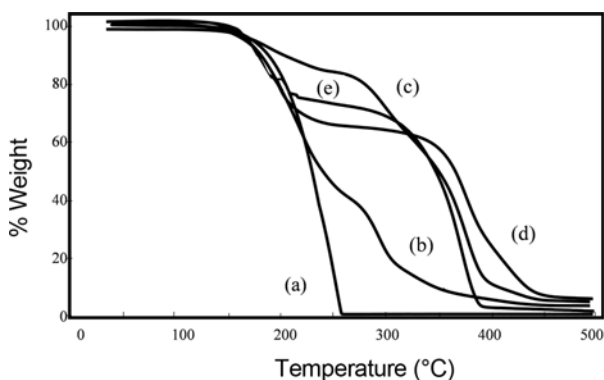


Figure 6. TGA thermograms of (a) pristine RT27 and microcapsules (after washed by 2-propanol) containing RT27 using GPLLA copolymerized with various comonomers and (b) GMA, (c) MMA, (d) EGDMA, and (e) PEGDA.

strength than the other types.

To determine the encapsulated RT27 content in microcapsule as $\%L_E$, the dried microcapsules were directly measured by TGA after washing with methanol. The degradation temperatures of a pristine RT27 (140-260 °C) and encapsulated

Table 2. Percentages of conversion, loading and encapsulation of RT27 in microcapsule prepared by microsuspension polymerization using polymer:RT 27 ratio of 50:50 with various comonomers

Comonomers	%Conversion	Loading (wt %)		% EE
		L_{th}^a	L_E^b	
GMA	100	50	48	96
MMA	100	50	15	30
EGDMA	96	53	42	79
PEGDA	81	55	36	66

^aCalculated by equation 2 and ^bthe percent weight loss of the encapsulated RT27 measured by TGA.

RT27 (130-260 °C) in microcapsules using copolymer between GPLLA and various comonomers (1:1 weight ratio) are shown in Figure 6. TGA measurement confirmed that RT27 existed in the prepared microcapsules. $\%L_E$ can be obtained from the percent weight loss of the encapsulated RT27 whose degradation temperature accorded with the pristine RT27. Based on a large number of broken particles for GPLLA copolymerized with MMA (Figure 6(c)), EGDMA (Figure 6(d)) and PEGDA (Figure 6(e)), the

obtained $\%L_E$ of those particles was lower than 42 % (Table 2). In the case of GMA, wherein the polymer shell completely envelops the RT27 core, $\%L_E$ (48 %) was close to the theoretical values ($\%L_{th}$ of 50 %) calculated in equation (2). In addition, the given $\%EE$ calculated from equation (3) was quite high at 96 %. This indicates that copolymerization of GPLLA and GMA provided high $\%EE$ for RT27. Therefore, GMA was selected for further experimentation.

It is well known that highly active primary radicals ($RO\cdot$) initiated from BPO can capture hydrogen at the α -carbon atom relative to the ester group from GPLLA [39]. GPLLA

macroradicals were obtained. Three possible reactions—recombination of two GPLLA macroradicals, recombination between GPLLA macroradical and PGMA homopolymer active chain, and GMA grafting onto GPLLA macroradical—may have occurred during the polymerization. To confirm the graft copolymerization between GPLLA and GMA, the polymerization was conducted again without RT27. Upon completion of the reaction, GPLLA-g-PGMA was purified by precipitation in methanol before drying overnight in a vacuum oven [39]. Approximately 80 % of GPLLA-g-PGMA was obtained. This indicates that the polymerization mainly occurred via a grafting reaction of GMA onto GPLLA chains. The FTIR spectra of GPLLA, GMA, and GPLLA-g-PGMA are shown in Figure 7. The spectrum of GPLLA (Figure 7(a)) indicated important absorption peaks at $3000\text{--}2940\text{ cm}^{-1}$ and $1190\text{--}1090\text{ cm}^{-1}$, which are associated with C-H stretching and O=C=O stretching vibrations, respectively. In the case of GMA's spectrum (Figure 7(b)), the wavenumbers of 910 cm^{-1} and 1650 cm^{-1} are attributed to the epoxy group asymmetric stretching and C=C stretching vibrations, respectively. All important absorption peaks presented in GPLLA and GMA spectra were observed in GPLLA-g-PGMA's spectrum (Figure 7(c)). In addition, the evident wavenumber of 910 cm^{-1} and the absence of wavenumber of 1650 cm^{-1} indicated that the GPLLA chain successfully grafted with GMA. In addition, $^1\text{H NMR}$ was also used to confirm the grafting reaction in which the $^1\text{H NMR}$ spectra of GPLLA, GMA and GPLLA-g-PGMA were overlaid as shown in Figure 8. It was found that the methine

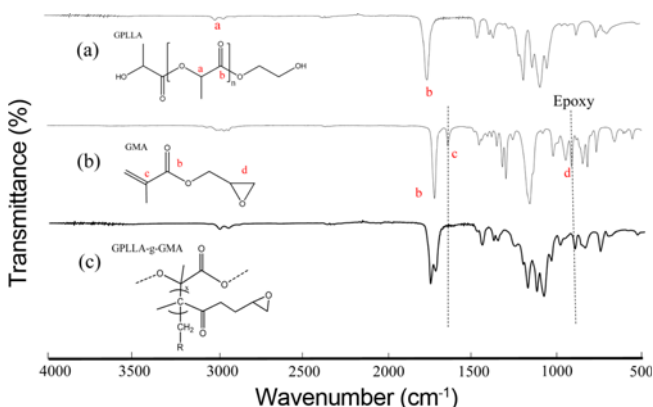


Figure 7. AIR-FTIR spectra of (a) GPLLA, (b) GMA, and (c) GPLLA-g-PGMA.

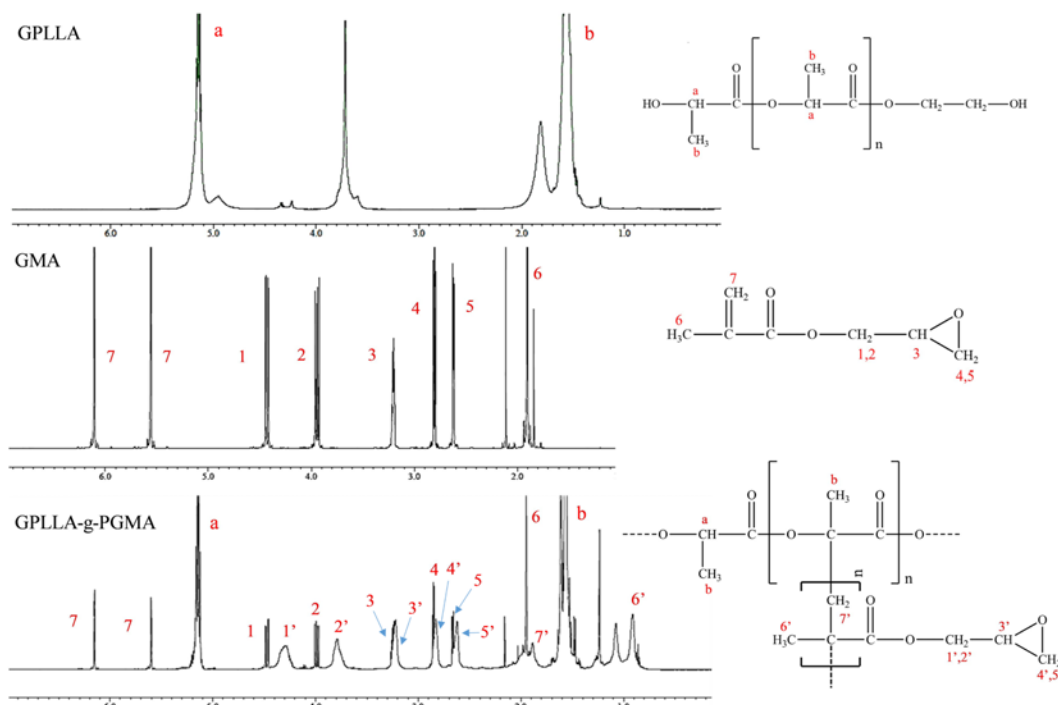


Figure 8. $^1\text{H NMR}$ spectra of GPLLA, GMA and GPLLA-g-PGMA.

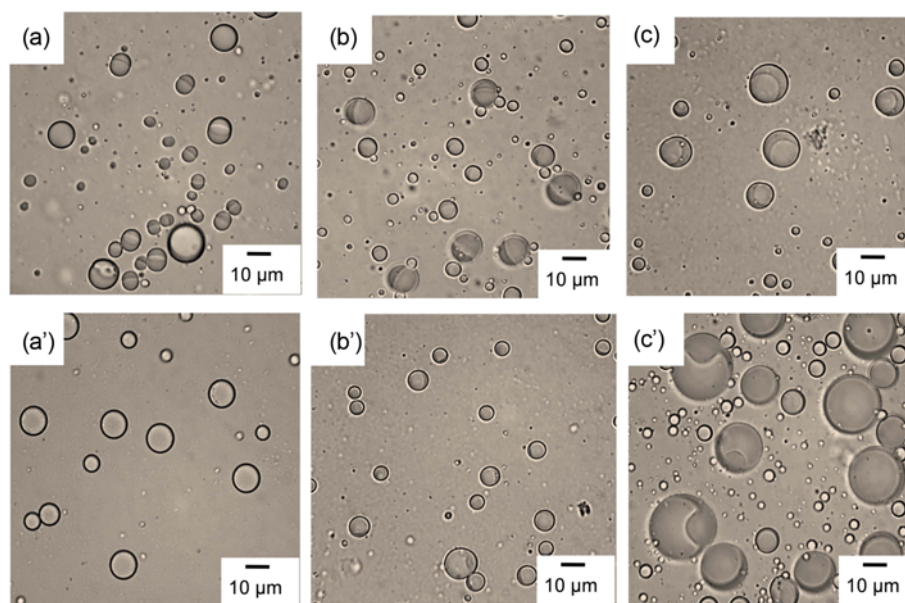


Figure 9. Optical micrographs of monomer droplets (a-c) and microcapsules containing RT27 (a'-c') prepared by microsuspension polymerization using various GPLLA: GMA ratios; (a, a') 1:1, (b, b') 3:2, and (c, c') 4:1.

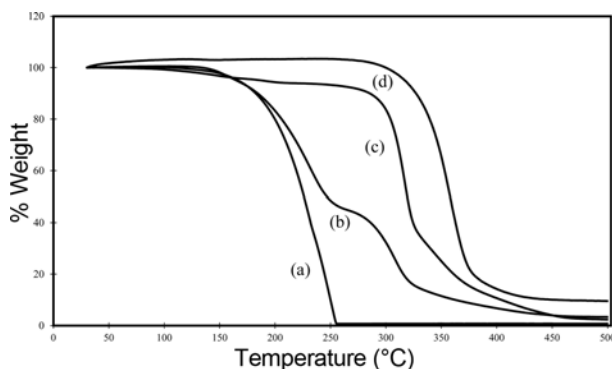


Figure 10. TGA thermograms of (a) pristine RT27 and microcapsules (after washed by 2-propanol) containing RT27 using various GPLLA:GMA ratios; (b) 1:1, (c) 3:2, and (d) 4:1.

and methyl protons of the GPLLA chain were observed at 5.2 and 1.6 ppm, respectively, of both GPLLA and GPLLA-g-PGMA spectra. GMA constitutional units of CH, CH₂ and CH₃ protons (1-7) were observed at 1.9-6.2 ppm for both GMA monomer and GPLLA-g-PGMA spectra where the intensity of those peaks was significantly decreased in the case of grafting polymer spectrum. Moreover, the new peaks at 0.9-4.3 ppm correspond to the protons 1'-7' of PGMA chain in GPLLA-g-PGMA were clearly observed. The chemical shifted of all peaks was due to the graft polymerization of PGMA onto the GPLLA chain [39,40]. However, the weaker peaks of methine (7) and methyl (6) protons of GMA observed in GPLLA-g-PGMA spectrum may indicate that GPLLA-g-PGMA chain was end-capped

by GMA via epoxide ring opening. These results accorded with FTIR analysis that the GMA successfully grafted onto the GPLLA chain.

To obtain highly eco-friendly microcapsules, the GPLLA content was increased from a GPLLA:GMA ratio of 1:1 to 3:2 and 4:1, whereas RT27 content was maintained at 50 %. The optical micrographs of monomer droplets and microcapsules of these three conditions are shown in Figure 9. Internal phase separation in the oil phase or monomer droplets increased with GPLLA content, as shown in Figure 9(b) and (c). After polymerization, acorn-like particles were observed in both cases (Figure 9(b') and (c')). Although they seemed stable in the suspension state, most of the microcapsules were broken after the washing and drying process. From TGA measurement (Figure 10(c) and (d)), %L_E of RT27 in microcapsules of GPLLA:GMA with ratios of 3:2 and 4:1 were only 15 and 2 wt%, respectively. This provides evidence that most of the obtained microcapsules were broken. In addition, their %EEs calculated from Equation 3 were 26 and 3 % for GPLLA:GMA with ratios of 3:2 and 4:1, respectively. Therefore, the maximum GPLLA amount for microcapsule preparation in this work was 50 wt% of the polymer shell.

The latent heats (J/g-sample) of encapsulated RT27 in microcapsules using a GPLLA:GMA ratio of 1:1 could be obtained by DSC measurement (Figure 11). Based on these results, the latent heats in the term of J/g-RT27 calculated by equation (1) were 202 and 200 J/g-RT27 for ΔH_m^* and ΔH_c^* , respectively, which approached the values of the pristine RT27 ($\Delta H_m=214$ and $\Delta H_c=210$ J/g). This result accorded with the high-performance PMMA shell where the latent

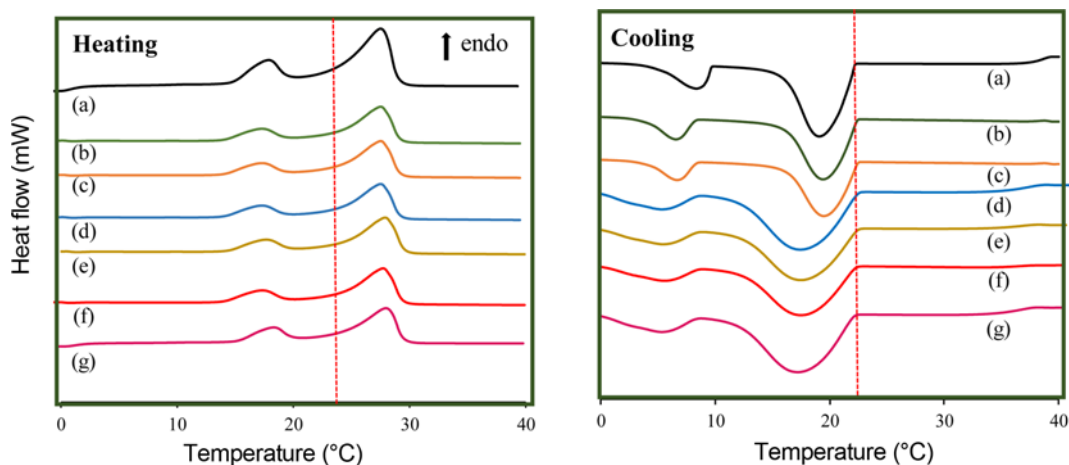


Figure 11. DSC thermograms of pristine RT27 (a) and GPLLA-g-PGMA/RT27 microcapsule at various thermal cycling tests (time); 0 (b), 10 (c), 20 (d), 30 (e), 40 (f), and 50 (g).

Table 3. Thermal properties of pristine RT27 and encapsulated RT27 in GPLLA-g-PGMA shell with various thermal cycling tests

Cycling (time)	Thermal properties			
	ΔH_m^* (J/g-RT27)	ΔH_c^* (J/g-RT27)	T_m (°C)	T_c (°C)
Pristine RT27	214	210	24	22
0	202	200	24	22
10th	190	187	24	22
20th	195	183	24	22
30th	192	189	24	22
40th	187	188	24	22
50th	192	189	24	22

heats of encapsulated RT27 were not different from the pristine RT27 [19]. These indicate that using GPLLA-g-PGMA shell the internal phase separation between the polymer shell and the RT27 core smoothly proceeded according to our proposals in previous articles [17,19]. In addition, the starting point T_m (24–25 °C) and T_c (22–23 °C) values of encapsulated RT27 were almost the same as those of pristine RT27. Moreover, the thermal properties of encapsulated RT27 with 50 melting/crystallizing cycles were investigated using DSC analysis as shown in Table 3 and Figure 11. It was found that throughout the thermal cycling study, the latent heats and phase change temperature almost maintained. When comparing the phase change temperatures (both T_m and T_c) at the starting point of RT27 encapsulated in the prepared microcapsule before thermal cycling and the 50th thermal cycling, the temperatures change only by 1.0 °C. In addition, the latent heats ($\Delta H_m^*=192$ and $\Delta H_c^*=189$ J/g-RT27) of the 50th thermal cycling decrease only 3–7 % and 6–9 % for ΔH_m^* and ΔH_c^* , respectively, from the

before thermal cycling. The very small changes in thermal properties indicated that the prepared microcapsules containing RT27 are thermally reliable.

In general, a supercooling phenomenon is observed in the case of microcapsules prepared by microsuspension polymerization [16–19,22,41–46]. The absence of supercooling in this work may be due to the fact that the obtained microcapsule size is quite large, so most particles may contain some impurities. Therefore, the crystallization of RT27 is normally nucleated based on heterogeneous nucleation in addition to homogeneous nucleation of the small size microcapsules. The general phenomenon was that supercooling decreased with the increase of particle size [47].

Conclusion

Bio-based spherical GPLLA-g-PGMA microcapsules encapsulated in RT27 were successfully prepared by microsuspension polymerization for the first time. Using MMA, EGDMA, and PEGDA as comonomers, internal phase separation between GPLLA and comonomer was clearly observed, resulting in incomplete encapsulation. The broken particles were obtained. In contrast, spherical microcapsules without broken particles were smoothly formed using GMA with the highest %EE. The possible mechanism is based on GMA grafting onto GPLLA macroradicals generated by H abstraction of the primary radical initiated by BPO. In addition, a small change of thermal properties of encapsulated RT27 after 50th thermal cycling test was obtained. High-performance PLLA-g-PGMA/RT27 microcapsules with thermal reliability, having high latent heats without supercooling, would be appropriate for various heat storage applications.

Acknowledgments

This work was supported by a Research and Researcher for industry (RRi) grant of the Thailand Research Fund (TRF; No. MSD60I0017) and STP Chem Solutions Co., Ltd. (given to P. S.). Special thanks are due to Dr. Utt Eiamprasert at the Chemistry Department, Faculty of Science and Technology, Rajamangala University of Technology Thanyaburi and The Rajamangala University of Technology Thanyaburi Instrumentation Center Laboratory for the ¹H-NMR facility.

References

- M. M. Farid, A. M. Khudhair, S. A. K. Razack, and S. Al-Hallaj, *Energ Convers. Manage.*, **45**, 1597 (2004).
- S. Mondal, *Appl. Therm. Eng.*, **28**, 1536 (2008).
- F. Agyenim, N. Hewitt, P. Eames, and M. Smyth, *Renew. Sustain. Energy Rev.*, **14**, 615 (2010).
- S. Sinha-Ray, R. Sahu, and A. Yarin, *Soft Matter*, **7**, 8823 (2011).
- A. Sharma, V. V. Tyagi, C. R. Chen, and D. Buddhi, *Renew. Sustain. Energy Rev.*, **13**, 318 (2009).
- Y. Zhang, X. Zheng, H. Wang, and Q. Du, *J. Mater. Chem. A*, **2**, 5304 (2014).
- Y. Ma, J. Zong, W. Li, L. Chen, X. Tang, N. Han, J. Wang, and X. Zhang, *Energy*, **87**, 86 (2015).
- Z. Jiang, W. Yang, F. He, C. Xie, J. Fan, J. Wu, and K. Zhang, *Langmuir*, **34**, 14254 (2018).
- Z. Chen, Y. Zhao, Y. Zhao, H. Thomas, X. Zhu, and M. Möller, *Langmuir*, **34**, 10397 (2018).
- H. Liu, X. Wang, and D. Wu, *ACS Sustain. Chem. Eng.*, **5**, 4906 (2017).
- X. Du, Y. Fang, X. Cheng, Z. Du, M. Zhou, and H. Wang, *ACS Sustain. Chem. Eng.*, **6**, 15541 (2018).
- S. Demirbağ and S. A. Aksoy, *Fiber. Polym.*, **17**, 408 (2016).
- R. Al-Shannaq, M. Farid, S. Al-Muhtaseb, and J. Kurdi, *Sol. Energy. Mat. Sol. C.*, **132**, 311 (2015).
- L. Sánchez-Silva, J. F. Rodríguez, A. Romero, A. M. Borreguero, M. Carmona, and P. Sánchez, *Chem. Eng. J.*, **157**, 216 (2010).
- A. Chaiyasat, S. Namwong, B. Uapipatanakul, W. Sajomsang, and P. Chaiyasat, *Int. J. Geomate*, **14**, 91 (2018).
- S. Namwong, M. Z. Islam, S. Noppalit, P. Tangboriboonrat, P. Chaiyasat, and A. Chaiyasat, *J. Macromol. Sci. A*, **53**, 11 (2016).
- P. Chaiyasat, S. Noppalit, M. Okubo, and A. Chaiyasat, *Sol. Energy. Mat. Sol. C.*, **157**, 996 (2016).
- S. Namwong, S. Noppalit, M. Okubo, S. Moonmungmee, P. Chaiyasat, and A. Chaiyasat, *Polym. Plast. Technol. Eng.*, **54**, 779 (2015).
- P. Chaiyasat, S. Noppalit, M. Okubo, and A. Chaiyasat, *Phys. Chem. Chem. Phys.*, **17**, 1053 (2015).
- L. Sánchez-Silva, J. F. Rodríguez, A. Romero, and P. Sánchez, *J. Appl. Polym. Sci.*, **124**, 4809 (2012).
- P. Sánchez, M. V. Sánchez-Fernandez, A. Romero, J. F. Rodríguez, and L. Sánchez-Silva, *Thermochim. Acta*, **498**, 16 (2010).
- D. Supatimusro, S. Promdsorn, S. Thipsit, W. Boontung, P. Chaiyasat, and A. Chaiyasat, *Polym. Plast. Technol. Eng.*, **51**, 1167 (2012).
- M. You, X. Wang, X. Zhang, L. Zhang, and J. Wang, *J. Polym. Res.*, **18**, 49 (2011).
- C. M. Free, O. P. Jensen, S. A. Mason, M. Eriksen, N. J. Williamson, and B. Boldgiv, *Marine Poll. Bull.*, **85**, 156 (2014).
- S. A. Carr, J. Liu, and A. G. Tesoro, *Water Res.*, **91**, 174 (2016).
- R. L. Shogren, W. M. Doane, D. Garlotta, J. W. Lawton, and J. L. Willett, *Polym. Degrad. Stabil.*, **79**, 405 (2003).
- D. Garlotta, W. Doane, R. Shogren, J. Lawton, and J. L. Willett, *J. Appl. Polym. Sci.*, **88**, 1775 (2003).
- T. Maharana, S. Pattanaik, A. Routaray, N. Nath, and A. K. Sutar, *React. Funct. Polym.*, **93**, 47 (2015).
- M. S. Abdelrahman, S. Nassar, H. Mashaly, S. Mahmoud, and D. Maamoun, *J. Adv. Chem.*, **15**, 6122 (2018).
- P. Chaiyasat, A. Chaiyasat, P. Teeka, S. Noppalit, and U. Srinorachun, *Energy Procedia*, **34**, 656 (2013).
- P. Chaiyasat, P. Pholsrimuang, W. Boontung, and A. Chaiyasat, *Polym. Plast. Technol. Eng.*, **55**, 1131 (2016).
- W. Boontung, S. Moonmungmee, A. Chaiyasat, and P. Chaiyasat, *Adv. Mat. Res.*, **506**, 303 (2012).
- M. Fashandi and S. N. Leung, *Mater. Renew. Sustain. Energy*, **6**, 14 (2017).
- P. Sangjun and A. Chaiyasat, "Seventh International Conference on Geotechnique, Construction Materials and Environment", p.505, Mie, Japan, 2017.
- T. Tanaka, R. Nakatsuru, Y. Kagari, N. Saito, and M. Okubo, *Langmuir*, **24**, 12267 (2008).
- J. Tounthai, A. Petchsuk, P. Opaprakasit, and M. Opaprakasit, *Polym. Bull.*, **70**, 2223 (2013).
- O. Torpanyacharn, P. Sukpuang, A. Petchsuk, P. Opaprakasit, and M. Opaprakasit, *Polym. Bull.*, **75**, 395 (2018).
- M. Tamizifar and G. Sun, *RSC Adv.*, **7**, 13299 (2017).
- J. Liu, H. Jiang, and L. Chen, *J. Polym. Environ.*, **20**, 810 (2012).
- E. Yoshida, *Polymers*, **4**, 1580 (2012).
- R. Al-Shannaq, J. Kurdi, S. Al-Muhtaseb, M. Dickinson, and M. Farid, *Energy*, **87**, 654 (2015).
- X. X. Zhang, Y. F. Fan, X. M. Tao, and K. L. Yick, *J. Colloid. Inter. Sci.*, **281**, 299 (2005).
- S. Jantang and P. Chaiyasat, *Fiber. Polym.*, **19**, 2039 (2018).
- P. Chaiyasat, M. Z. Islam, and A. Chaiyasat, *RSC Adv.*, **3**, 10202 (2013).
- P. Chaiyasat, A. Chaiyasat, W. Boontung, S. Promdsorn, and S. Thipsit, *Mater. Sci. Appl.*, **2**, 1007 (2011).
- P. Chaiyasat, Y. Ogino, T. Suzuki, and M. Okubo, *Colloid Polym. Sci.*, **286**, 753 (2008).